King Saud University

Arabian Journal of Chemistry

www.ksu.edu.sa
www.sciencedirect.com

ORIGINAL ARTICLE

Tailored surface silica nanoparticles for blood-brain barrier penetration: Preparation and *in vivo* investigation

B.I. Tamba [a,b,c,*], **V. Streinu** [a], **G. Foltea** [a], **A.N. Neagu** [d], **G. Dodi** [a,e], **M. Zlei** [f], **A. Tijani** [g,h], **C. Stefanescu** [a]

[a] *"Grigore T. Popa" University of Medicine and Pharmacy, 700115 Iasi, Romania*
[b] *Oxygen Handel Gmbh, 68219 Mannheim, Germany*
[c] *A&B Pharm Corp, 611075 Roman, Romania*
[d] *"Alexandru Ioan Cuza" University of Iasi, 700506, Romania*
[e] *SCIENT – Research Centre for Instrumental Analysis, 077167 Bucharest, Romania*
[f] *Regional Oncology Institute, 700483 Iasi, Romania*
[g] *NanoSERVE, c/o Institute Pasteur de Lille, 59019, France*
[h] *FHNW, School of Life Sciences, CH-4132, Switzerland*

Abstract   Surface modified fluorescent silica nanoparticle derivatives (Ru@SNPs), namely, glucose (Glu) and glucose-poly (ethylene glycol) methyl ether amine (Glu-PEG) coated SNPs were designed and tested for their ability to penetrate the blood-brain barrier (BBB) in mice brain. The new obtained nanoparticles were characterized by field emission scanning electron microscope (FE-SEM), dynamic light scattering (DLS) and Fourier transform infrared (FTIR-ATR) analysis. The BBB penetration and distribution of tailored SNPs in mice brain were examined using confocal laser scanning microscopy (CLSM), flow cytometer (FACS) and transmission electron microscopy (TEM). The promising results obtained by *in vivo* experiments, point out that silica nanoparticle derivatives are an efficient permeable delivery vehicle that are able to cross the BBB and reach the brain tissues *via* specific and non-specific mechanisms. These findings will enrich the knowledge to rationally engineer multifunctional nanoparticles, and bring new insights into BBB permeability.
© 2018 The Authors. Production and hosting by Elsevier B.V. on behalf of King Saud University. This is an open access article under the CC BY-NC-ND license (http://creativecommons.org/licenses/by-nc-nd/4.0/).

* Corresponding author at: "Grigore T. Popa" University of Medicine and Pharmacy, 700115 Iasi, Romania.
  E-mail address: bogdan.tamba@umfiasi.ro (B.I. Tamba).
Peer review under responsibility of King Saud University.

ELSEVIER | **Production and hosting by Elsevier**

1. Introduction

The blood-brain-barrier (BBB), a dynamic and extremely complex interface between the blood and the central nervous system (CNS), is composed mainly of endothelial cells, from the brain capillaries united by tight junctions, luminal glycocalyx,

basal lamina and astrocytic foot processes (Das et al., 2016). The endothelial cells of the brain microvessel display important morphological characteristics, such as the presence of tight junctions between the cells, the absence of fenestrations and a diminished pinocytic activity. Together it controls the passage of molecules from the circulatory system into the brain, protecting it from the invasion of various harmful compounds (Gomes et al., 2016). The complex tight junctions of the cerebral endothelium form also a continuous lipid layer that allows passage of only small, electrically neutral, lipid-soluble molecules. In addition, the endothelial cells possess extremely efficient efflux transporters that pump back into the blood stream most of the drug molecules by ATP binding cassette C1 (ABCC1) and ABCB1 (known also as p-glycoprotein) present in the luminal plasma membrane of brain microvessel endothelial cells (Abbott et al., 2006; Barua and Mitragotri, 2014). Under normal conditions, the BBB acts as an impermeable membrane to toxic agents that defends the integrity of the brain, but also obstructs the delivery of diagnostic and therapeutic agents to the brain (Singh et al., 2017).

According to previous research efforts available in the literature, several strategies have been developed to circumvent the BBB and to deliver drugs to the brain, including invasive and non-invasive techniques, such as disruption, direct administration of drugs by intraventricular infusion and intracerebral implants, BBB opening via ultrasound and electrical stimulation, inhibition of efflux transporters, osmotic opening of the BBB, prodrugs, etc. (Kanwar et al., 2012; Singh et al., 2015). All the proposed techniques are constrained by the limitations of this impermeable membrane barrier to conventional drug delivery systems such as tight capillary endothelial cells, enzyme clusters, the existence of efflux pumps receptors and transporters (Alexa et al., 2015; Cupaioli et al., 2014; Liu et al., 2014). However, the development of revolutionized delivery and diagnostic agents with rational features that will allow easy cellular permeation and controlled drug release still remains a crucial task for neurological pathologies (Chen and Liu, 2012; Fiandra et al., 2015).

One of the few possibilities to introduce into the brain drugs that would normally not be able to cross the BBB is the design of advanced targeted nanocarriers (Lalatsa and Barbu, 2016; Saraiva et al., 2016). Ideally, a balanced design of the nanocarrier should certify biocompatibility, a long circulation time in the bloodstream and ability to target the endothelial cells of the brain capillary, generating a local pharmacological action, with decreased side effects, a typical drawback of current therapies (Balan and Verestiuc, 2014; Mangraviti et al., 2016).

In the last decade, nanoparticles have received great attention over the usual strategies regarding transportation of drugs through BBB due to their versatile architecture, size, shape, flexibility, chemical surface features, as well as their stability, biodegradability, biocompatibility and biodistribution (Bharadwaj et al., 2018; Silva, 2008; Toman et al., 2015).

It has been shown that the material features, as well as nanoparticle size (Fornaguera et al., 2015) and surface modifications, among other factors, affect their mode of internalization by the endothelial cells of the brain microvessels and thereby, their subcellular fate and potential of crossing the epithelial cells of the BBB (Georgieva et al., 2014; Hanada et al., 2014).

The recent literature data reports several types of NPs which easily pass and transport drugs through BBB. For instance, a study of the transport efficiency of fluorescent poly-butylcyanoacrylate (PBCA) NPs over the BBB in animals showed that successful passage was achieved if NPs were fabricated with non-ionic surfactants or cationic stabilizers, concluding that the particle surface is the key factor determining BBB penetration. Neither the size nor chemo-electric charge of the NPs had any influence on BBB passage (Voigt et al., 2014). Also, Jose et al. (2014) reported that polysorbate 80 surface modified poly (lactic-co-glycolic acid) (PLGA) nanoparticles could be successfully developed for the brain delivery of neuroprotective drugs in the treatment of neurodegenerative disorders. The spherical-shaped PLGA nanoparticles coated with 1% polysorbate 80 were able to deliver 10-fold more Bacoside-A into the brain when compared to the free drug solution.

Compared with the above nanocarriers, silica nanoparticles (SNPs) are of great interest due to their versatile properties, such as relatively low cost production, high loading capability, large surface area and multifunctionalized anchoring features using different moieties, specifically, polyethylene glycol, amine, carboxyl or vinyl, rendering them useful for drug-delivery applications (Feng et al., 2016). Previous research studies focused on conjugating drug molecules to brain-specific transporters, namely, glucose, oligonucleotides, amino acids, PEG, that will enhance their penetration into the BBB, improve the plasma residence time and reduce clearance by the reticulo-endothelial system (RES). For example, Ku et al. (2010) synthesized PEGylated fluorescein-doped magnetic SNPs and evaluated their ability across the BBB and distribution in rat brain. The authors demonstrated that PEG molecule attached to the SNPs determined the penetration of the BBB and distribution inside the cytoplasm of vascular endothelial cells, the foot processes of astrocytes, and more important inside the cylindraxile of neurons. Liu et al. (2014) investigated the transport of SNPs through the BBB with a special interest on particle size. The authors evaluated *in vitro* and *in vivo* PEGylated SNPs of three different sizes, namely, diameters of 100, 50, and 25 nm. The results indicate that PEG-SNPs transport efficiency and brain uptake increases when the particle size decreases. Even though, an ideal molecule has not yet been designed, significant research has been done to personalize nanotechnology delivery strategies for crossing the BBB (Caruso et al., 2011).

Taking into consideration the above mentioned potential solutions and current drawbacks, the main objective of this study was to design new brain "tailor-made" nanoparticles and evaluate them *in vivo* on experimental mice across the BBB at the cellular and subcellular level using specific techniques. To the best of our knowledge, this strategy has not been yet reported in the literature.

2. Material and methods

TEOS (tetraethyl orthosilicate), florescent dye $Ru(bpy)_3Cl_2$ (tris (bipyridine) ruthenium (II) chloride) (Ru), 3-(triethoxysilyl) propyl isocyanate (TESPIC), glucose (Glu), poly(ethylene glycol) methyl ether amine (PEG-NH_2), Triton X100, n-hexanol, cyclohexane, aqueous ammonia solution (NH_3, 28–30%), and ethanol (> 99.9%) from were acquired

from Sigma Aldrich. All solutions were prepared with ultra-pure water (18.2 MΩ·cm).

The fluorescent $[Ru(bpy)_3]Cl_2$ dye marker was entrapped in SNPs in order to visualize and monitor the nanoparticles that cross the BBB.

Three types of SNPs derivatives were synthesized and used for *in vivo* evaluation, as follows:

– Batch Ru@SNP: fluorescently labeled mono-shell silica nanoparticles were prepared by the reverse microemulsion method previously described in another paper (Legrand et al., 2008). Typically, in a mixture of Triton X100 (2.92 mM, 2.04 equiv.), n-hexanol (1.43 mM, 1 equiv.) and cyclo-hexane (69.4 mM, 48.5 equiv.), 100 mL of an aqueous solution of $[Ru(bpy)_3]Cl_2$ (1.34 mM) was added. After magnetically stirring the mixture for 30 min, TEOS (0.45 mM, 0.32 equiv.) was added, followed by 60 mL of ammonia. The reaction was allowed to proceed for 24 h, then 10 mL of acetone were added to break down the microemulsion; the colloidal silica nanoparticles were isolated *via* centrifugation and washed several time with ethanol and water.
– Batch Ru@Glu-SNP: the glucose-coated silica nanoparticles were obtained using 50 mg of Ru@SNP suspended in 10 mL of ultrapure water under sonication. To this suspension, 15 µL of (3-(triethoxysilyl) propyl isocyanate were added dropwise under stirring at room temperature. The stirring was continued overnight. The isocyanate-functionalized fluorescent Ru@SNP were collected by centrifugation and washed with water several times to remove the unreacted species. The colloidal nanoparticles were dried at 60 °C under low pressure and then immersed into 10 mL of aqueous glucose solution (5 mg/mL) and stirred for 6 h. The glucose coated Ru@SNP were isolated and kept for further steps.
– Batch Ru@Glu-PEG-SNP: the PEGylated glucose-coated SNPs were obtained using the same procedure as for the preparation of Ru@Glu-SNP, except that the glucose solution was mixed with 100 mL of PEG-NH₂ before immersion of fluorescently labelled nanoparticles.

Characterization of the SNP derivatives: FE-SEM experiments were carried out at an accelerating voltage of 20 kV on a field emission scanning electron microscope (FE-SEM, Zeiss, SUPRA VP 40). Samples suspended in ultrapure water (1 mg/mL) were deposited on freshly cleaved mica surface, dried and gold/palladium coated. Determination of nanoparticles size, and polydispersity index were performed using a Zetasizer (Zetasizer Nano ZS, Malvern Instruments). The samples were dispersed in physiological media and measured at a scattering angle of 90° and 25 °C. Qualitative chemical composition assessment of composite particles was performed by FTIR-ATR analysis (Frontier, Perkin Elmer).

Experimental animals: All animals experimental procedures employed in the present study were strictly in accordance with the European Community Guidelines regarding ethics and approved by "Grigore T. Popa" University of Medicine and Pharmacy animal care and use committee (No.610/06.01. 2017). The animal breeding facility supplied adult male Swiss mice with an average weight of 20 g ± 2 g. The animals were housed in a temperature-controlled room (21 °C ± 2 °C) with a 12/12 h light/dark cycle, 4 mice per cage, and allowed to

acclimate for at least 24 h before use, and given food and water ad libitum.

Qualitative cellular uptake analysis by confocal microscopy: Fluorescent silica nanoparticle derivatives (batches Ru@Glu-SNP and Ru@Glu-PEG-SNP) (1 mg/1 mL in 10% glucose solution, sonication for 30 min) were administered intraperitoneally (0.2 mL/mouse) to test group of 6 mice. The control group (6 animals) received a similar volume of glucose solution. At 1 h after administration the mice were deeply anesthetized with xylazine and transcardially perfused with 15 mL 0.9% saline solution, followed by fresh 4% paraformaldehyde (PFA) in 75 mL 0.1 M PBS. The whole brain was extracted and post-fixed overnight in 4% PFA, followed by cryoprotection in 30% sucrose in PBS for 72 h. Coronal sections of the above mentioned organ were cut using a freezing microtome (CM 1850 Leica Microsystems, Germany), collected and mounted on slides and examined in a Leica Confocal Laser Scanning Microscope (TCS SPE DM 5500Q), using a laser diode (480 nm excitation and 610–630 nm emission).

Brain uptake study by flow cytometer analysis: Fluorescent silica nanoparticles (batches Ru@Glu-SNP and Ru@Glu-PEG-SNP) were suspended at a concentration of 1 mg/mL in 10% glucose solution and sonicated for 30 min. After ultrasonication, the nanoparticle suspensions were administered intraperitoneally (0.2 mL/mouse) to a test group of 6 mice. The control group (6 animals) received a similar volume of glucose solution. In order to remove the circulating nanoparticles, transcardiac perfusion with Ringer solution was performed and within 1 h after nanoparticles administration, the brains where harvested. The mice were deeply anesthetized with xylazine and sacrificed. The brain tissues were homogenized using mechanical processing and incubated for 30 min with 2 mL cell lysing solution (radioimmunoprecipitation assay (RIPA) buffer that contains 50 mM TRIS, 150 mM NaCl, 1% Triton X-100, 0.5% sodium deoxycholate and 0.1% SDS). Brain tissues samples were centrifuged (15000 rpm, 5 min) and the supernatants (1 mL/sample) were removed, diluted with 1 mL distilled water, and analysed by flow cytometer using a FACS Canto II machine (BD Bioscience). The SNPs were detected based on their fluorescence properties using a 488 nm/670 nm LP PMT detector. Dual dot plots depicting characteristics of red fluorescence versus side scattered light for nanoparticles (batches Ru@Glu-SNP and Ru@Glu-PEG-SNP), brain control samples and brain samples injected with the nanoparticles are presented.

Transmission electron microscopy of brain tissue sections: To determine the localized biodistribution of nanoparticles in brain tissues, the sections were examined by TEM (Zeiss EM- 900, resolution of 0.5 nm) operating at 80 kV. Brain tissues were excised at 1 h after SNPs administration (batch Ru@Glu-PEG-SNPs), harvested, fixed in glutaraldehyde and post-fixed in osmium tetroxide. After dehydration, tissue samples were embedded in Epon. Ultrathin sections were mounted on copper grids and stained with uranyl acetate and lead citrate and examined by TEM.

3. Results and discussion

This study aimed to design different types of SNP suitable for intraperitoneal administration and for BBB targeting. The

nanoparticles had to accomplish several requirements, such as nanometric size (below 1 μm) to avoid embolization, stability after reaching the target site, and physicochemical properties that facilitate their BBB passage. The production of brain "recognizing" nanoparticles with effective targeting through surface modification revolutionizes modern therapeutics due to the possible preferential recognition of specific cells, facilitating binding and affinity-based endocytosis (Craparo et al., 2011). This has been accomplished using a low-cost, low-energy, improved approach, not yet used in the context of BBB permeability research: reverse emulsion pattern of silica shell well known to provide good biocompatible, non-toxic coating as well as a hydrophilic surface. The production of the tailored surface SNPs via a multistep procedure is illustrated in Fig. 1, which involves synthesis of fluorescent SNPs, glucose deposition and PEG-functionalization onto the silica surface. In detail, first, fluorescent mono-shell silica nanoparticles were successfully synthesized by a slightly modified water-in-oil microemulsion procedure as reported in a previous paper regarding batch Ru@SNP (Legrand et al., 2008). The silanol group on the SNPs can be easily modified to link bioconjuga-

tors by different methods with specific biofunctionalities. Therefore, we systematically changed the surface chemistry of the obtained nanoparticles by the introduction of isocyanate groups in the second shell-growth (Ru@Iso-SNPs), followed first by glucose coating for increased binding affinity with different cell surfaces (batch Ru@Glu-SNP). Secondly, the SNPs were reacted with glucose and PEG to produce a biologically functionalized surface of the multi-shell nanoparticles (batch Ru@Glu-PEG-SNP). Previous research reports presented that SNPs modified with PEG can enhance the plasma residence time and reduce clearance by RES, increase the endothelial permeability of NPs and thus facilitate their BBB passage (Chen and Liu, 2012).

Physical characterization of SNPs obtained under a variety of conditions was performed by using FE-SEM, presented in Fig. 2 through a series of images. As revealed in this figure the nanoparticles exhibited sphere-shaped features with uniform size and smooth exterior. Fig. 2A shows the typical surface structure of unmodified Ru@SNPs with a diameter of approximately 70 nm, the tendency to form "grape-like morphology" in dry-state, as a result of the Van der Waals and
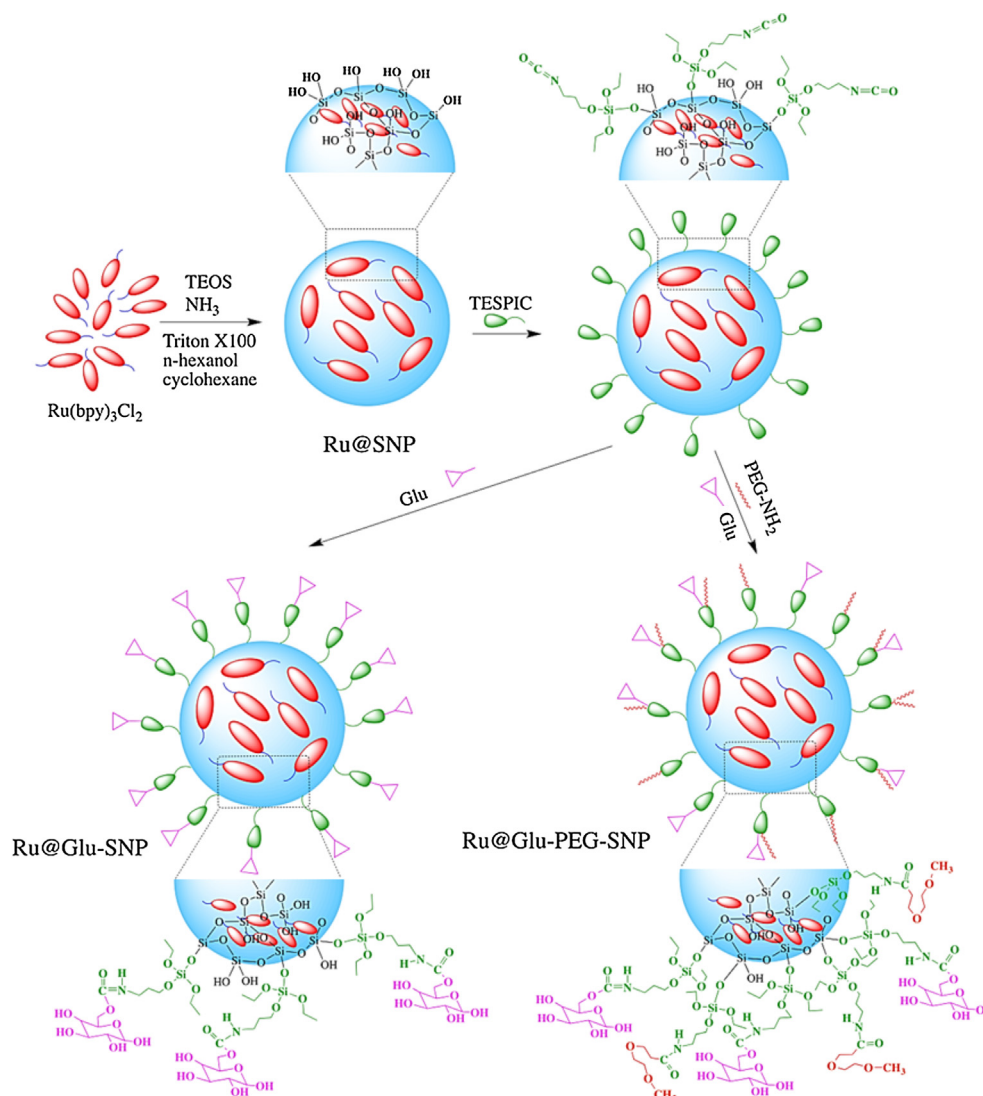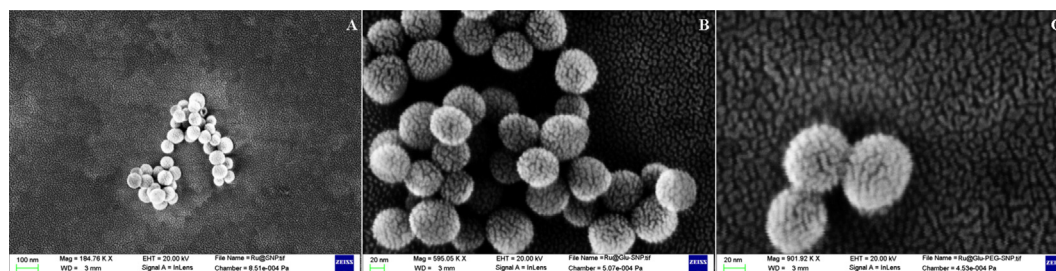

**Fig. 1** Synthesis strategy for Ru@SNPs, Ru@Glu-SNPs and Ru@Glu-PEG-SNPs.

Fig. 2 SEM micrographs of A. Ru@SNPs produced without surface modification, B. glucose modified particles (Ru@Glu-SNPs) and C. PEG-modified particles (Ru@Glu-PEG-SNPs).

other inter-particle forces closely correlated with the very high surface area to volume ratio. This type of behaviour was expected from the synthetic method, where the probability of the growing nanoparticles contacting each other is relatively low. After the second shell addition (batch Ru@Glu-SNP), the geometry of the particles was not altered, glucose had no influence on the SNPs size. Fig. 2B shows that the nanoparticles are not bridged, and we believe that the bulk of the material is in this form. Some interesting features were observed on the third SNPs category, batch Ru@Glu-PEG-SNP (Fig. 2C), where the nanocarriers have the tendency to form highly ordered two-dimensional arrays on mica, closely resembling a triangle close packing. The diameter was estimated to be also around 70 nm.

These types of conformation rise out the question: whether such aggregated structures are formed also in physiological fluids, since, aggregation might drastically affect their capacity to cross BBB. It is well known that the brain uptake increases when particle size decreases, therefore, the size distribution, zeta potential and polydispersity index in physiological media of the synthesized nanoparticles were determined. In agreement with FE-SEM results, dynamic light scattering measurements evidenced (Fig. 3) the hydrodynamic diameter when dispersed in physiological solution with values in the range of 60–80 nm. In contrast with FE-SEM, the characterization of the hydrodynamic properties does not show agglomerates for these samples under physiological conditions, suggesting that only dry preparation of colloidal samples induces aggregations. The larger diameter of the bare Ru@SNPs might be explained by the polydispersity of the sample and indirectly confirms the presence of small aggregates formed in the presence of physiological media due to particles highly polar behaviour. In the presence of glucose, the Ru@Glu-SNPs tended to stabilize at 71 nm and this suggests that the added thin layer modulates the silica surface. However, after the addition of PEG to the SNPs surface (Ru@Glu-PEG-SNPs) a steady state was established, the mean particle diameter and polydispersity were constant, mainly due to the fact that PEG remains the most important factor for steric colloidal stability (Rabanel et al., 2014).

The zeta potential measurements were performed in order to evaluate the surface properties of the produced SNPs. As expected, $Ru(bpy)_3^{2+}$-doped silica (Ru@SNPs) showed negative zeta potential values (−26.1 mV) due to the silanol groups.
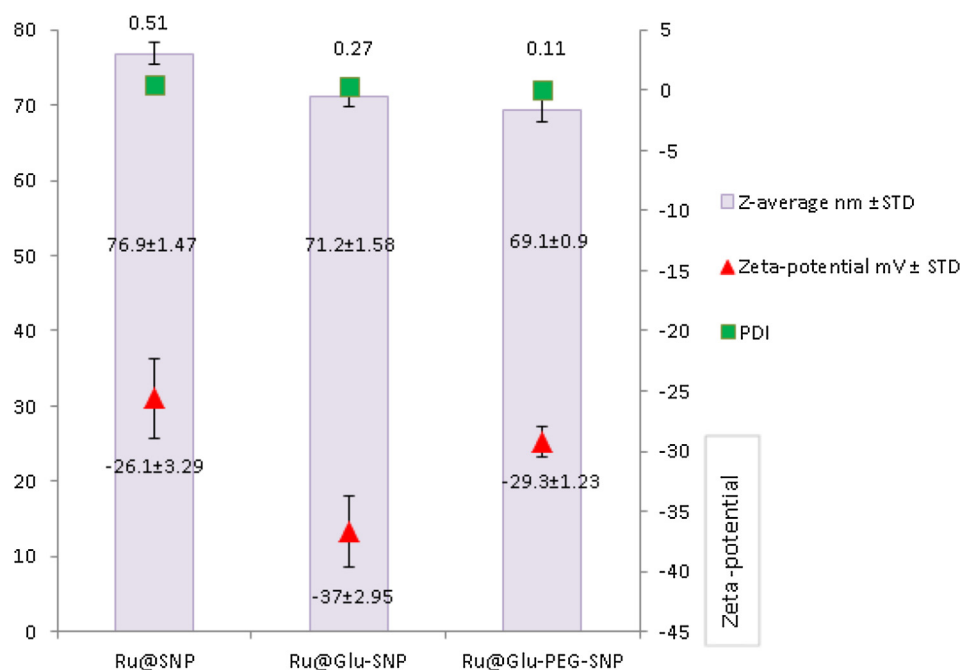
Fig. 3 Size distribution, zeta potential and polydispersity index of Ru@SNPs and derivatives.

Upon reaction with glucose, the zeta potential reached a negative value of -37 mV, which is attributed to the abundant hydroxyl groups which belong to glucose moieties on the nanoparticle surface. The introduction of PEG on SNPs surface determined a less negative value (−29.3 mV) which could be explained by the fact that, the additional PEG layer shields the underlying negative charges. The results obtained clearly indicated that the particles are fairly stable due to the electrostatic repulsion.

Surface chemistry (FTIR-ATR) analysis evidenced the formation of Ru@SNPs and the following derivatives, namely glucose modified particles (Ru@Glu-SNPs) and PEG-modified particles (Ru@Glu-PEG-SNPs) in the range of 400–4000 cm^{-1}. As can be seen in Fig. 4, pure doped silica particles (Ru@SNPs) possess characteristic peaks attributed to Si–O–Si bending (468 cm^{-1}), Si–O–Si symmetric stretching (802 cm^{-1}), external Si–OH groups (951 cm^{-1}), Si–O–Si asymmetric stretching (1095 cm^{-1}), –OH stretching (3468 cm^{-1}) and the characteristic absorption of Ru(bpy)$_3$Cl$_2$ molecules retained by siliceous materials (1629 cm^{-1}) (Zhou et al., 2013). The intermediate step represented by the efficient reaction between surface silanol and isocyanate groups was evidenced by ATR peaks related to isocyanate chains (2227 cm^{-1}). After modification with glucose, the SNPs still retained its siliceous structure, displaying no major changes in the formation of Ru@Glu-SNPs. The interaction of Ru@Iso-SNPs with glucose and PEG-NH$_2$ products was also confirmed by

ATR spectra (Fig. 4). Intense absorptions are observed at 1061, 1353, 1446 and 2369 cm^{-1}. The IR band at 1061 cm^{-1} is characteristic to the C–O stretching mode, 1456 and 1353 cm^{-1} bands due to C–H bending and 2369 cm^{-1} for the C–H stretching of the PEG chains (Ru@Glu-PEG-SNPs).

3.1. In vivo transport of SNPs across BBB

The BBB is an anatomic barrier developed to limit the penetration not only of harmful substances but also of drugs and other pharmacological compounds. Different research groups mentioned a variety of pathways for BBB penetration (Voigt et al., 2014). Crossing the BBB is based on both specific and nonspecific interactions between molecules and the BBB, on their receptor or absorptive mediated transcytosis by endothelial cells, opening of the tight junctions and inhibition of the transmembrane efflux systems, as well as other transcellular transport processes: paracellular or carrier-mediated transport (Grover et al., 2013). Given the presence of this complex selective network, the development of "tailor-made carriers" that can cross the BBB and efficiently deliver drugs to specific areas represent a vast achievement towards brain research.

Successful passage across the BBB was achieved with glucose and PEG coated nanoparticles via intraperitoneal route. To confirm the transport of SNPs with different surface chemistry (glucose modified nanoparticles (Ru@Glu-SNPs) and PEG-modified nanoparticles (Ru@Glu-PEG-SNPs)) across
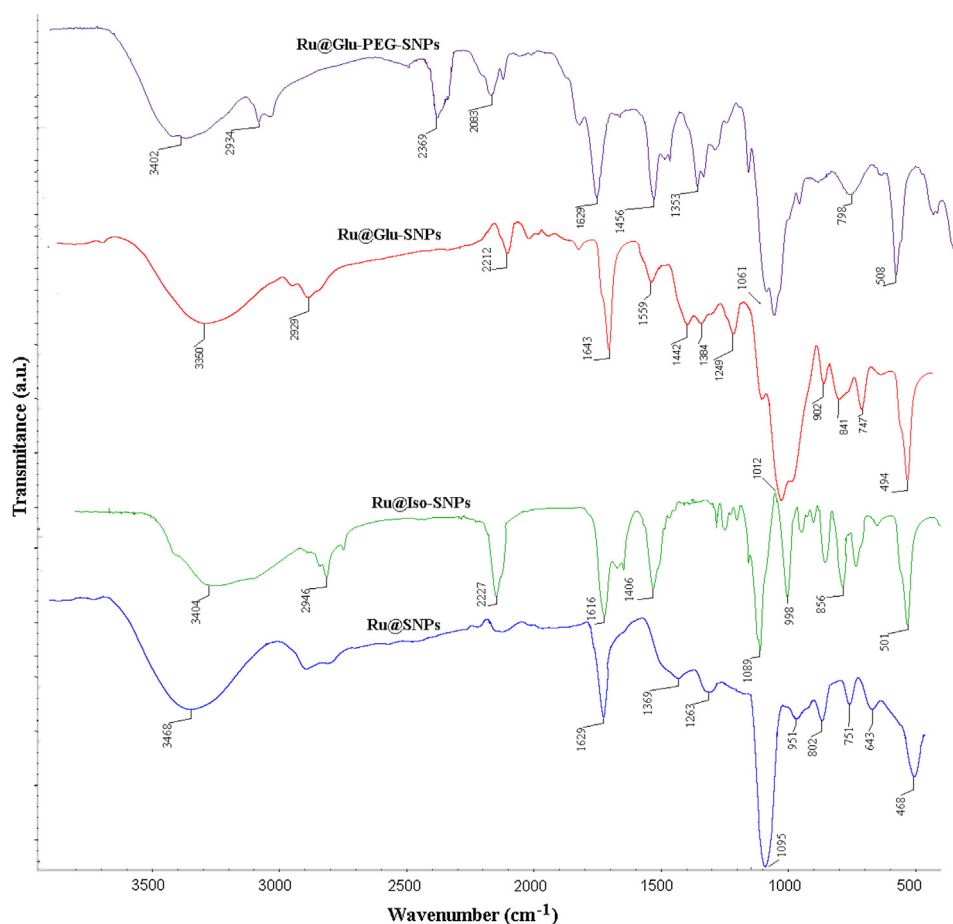

Fig. 4 Fourier transform infrared spectra for Ru@SNPs derivatives.

the BBB, the animals were further analysed by confocal microscopy. The results of the mice brain biodistribution are shown in Fig. 3, as indicated by the fluorescence signal of Ru(bpy)$_3$Cl$_2$ entrapped into the administered SNPs. Biodistribution studies revealed that the Ru@Glu-SNPs and Ru@Glu-PEG-SNPs exhibited a significant uptake in the brain region when compared with the control brain (Fig. 5A) or control SNPs (Fig. 5B and C) at 1 h post-administration. These results depicted in Fig. 5D and 5E illustrate the fluorescence emitting distribution of the administered nanoparticles in the brain coronal section.

In the case of PEGylated nanoparticles (Ru@Glu-PEG-SNPs), the fluorescence signal of Ru(bpy)$_3$Cl$_2$ dye from the brain 1 h post-injection was greatly increased with an obvious distribution, indicating that PEG modified glucose-SNPs have higher transport efficiency across the BBB than glucose SNPs. It is well known that the mechanisms underlying BBB passage may depend on various factors, namely, size, electric charge, surface molecules, and specific interactions with the endothelial cells. Therefore, the higher permeability of the PEG-modified NPs could be explained by the different surface-charge according to Hanada et al. (2014) that specifies that the cationic amino-NPs tend to be transported onto the baso-lateral side through the BBB model with higher permeability than anionic carboxyl- or neutral NPs. In our study, the PEG amino SNPs (batch Ru@Glu-PEG-SNPs) probably interact with the cell anionic phospholipidic surface and were transported through the BBB by paracellular pathway. Also, it has been assumed that SNPs adsorb apolipoprotein E (apoE) transporters in plasma onto their surfaces and cross the BBB via receptor-mediated transcytosis (Koffie et al., 2011) due to their biodegradability and surface moieties. Transcytosis in endothelial cells starts with internalization of SNPs into the cells by vesicular carriers, then subsequently processed via different pathways to appropriate intracellular organelles and recycled, degraded, or transcytosed to the contralateral side.

The BBB also holds a number of transport proteins, such as the glucose transporter (GLUT) essential for the permeation of nanocarriers. Therefore, we assume that the glucose modified SNPs were recognized by the GLUT protein and transported into the brain endothelium through carrier-mediated transport. The role for GLUT in the transport of the nanoparticles across the BBB was confirmed in a previous study by Jiang et al. (2014) where glucose-modified paclitaxel-loaded polymeric nanoparticles were successfully employed in the treatment of intracranial glioma in mice.

Based on the data discussed in the present work, we can consider that SNPs drug delivery systems for the brain act like "Trojan horses", and therefore, reflect the existence of a novel vehicle technology for the BBB permeability (Wohlfart et al., 2012).

3.2. Flow cytometry for in vivo uptake evaluation

To further quantify the brain cells which internalized the nanoparticles, we performed flow cytometry on homogenized brain tissue samples 1 h after administration. Flow cytometry allowed us a rapid, multiparametric analysis with robust statistics due to large number of events measured in 3D. By using fluorescently labelled nanoparticles it was possible to qualify and semiquantify their internalization in brain tissues by FACS (Fluorescence-activated cell-sorting). Therefore, in the dot plots, X-axis reflects the fluorescence intensity in logarithmic scale, and Y-axis corresponds to the side scatter (SSC-A) intensity in linear scale. Fig. 6 presents FACS analysis of the
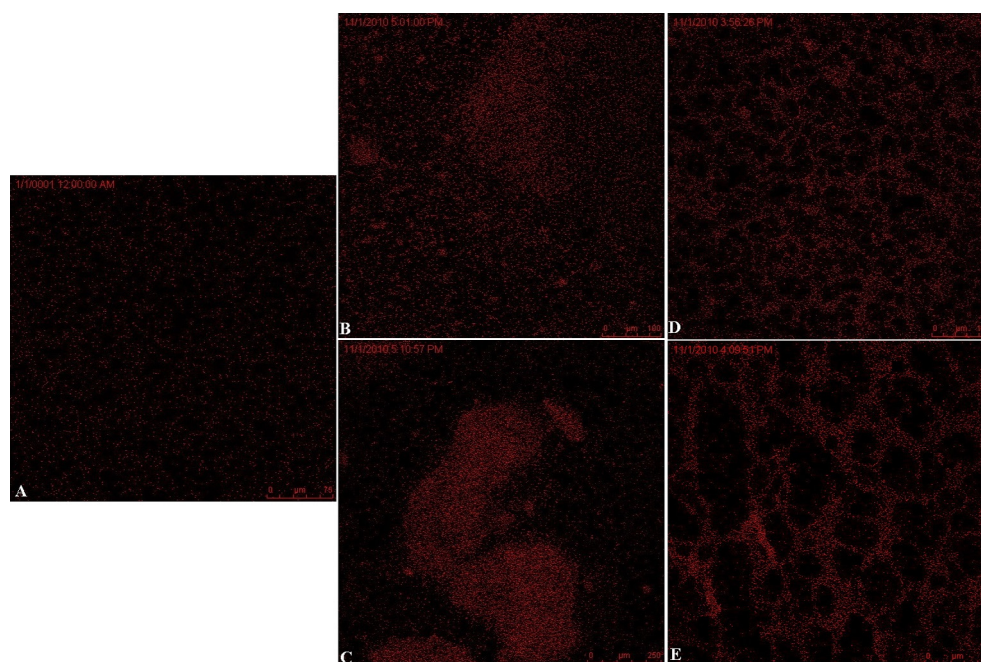
Fig. 5 Confocal fluorescence images of: A. Brain Control, 10×20; B. Control solution of glucose modified particles (Ru@Glu-SNPs), 10×20; C. Control solution of PEG-modified particles (Ru@Glu-PEG-SNPs), 10x20; D. Brain mice with Ru@Glu-SNPs, 10×20; E. Brain mice with Ru@Glu-PEG-SNPs; 10×20.
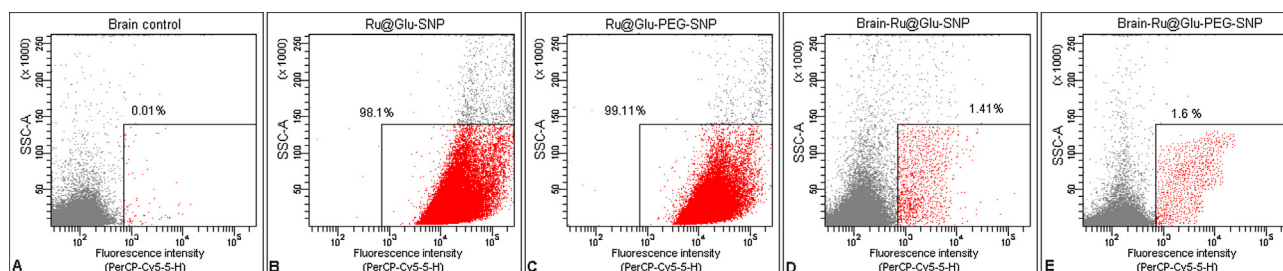
Fig. 6 FACS analysis of: A. Brain Control, 10 × 20; B. Control solution of glucose modified particles (Ru@Glu-SNPs), 10 × 20; C. Control solution of PEG-modified particles (Ru@Glu-PEG-SNPs), 10 × 20; D. Brain mice with Ru@Glu-SNPs, 10 × 20; E. Brain mice with Ru@Glu-PEG-SNPs; 10 × 20.

brain control sections, control solution of the tested SNPs and brain sections containing SNPs. The fluorescence emissions from the SNPs are shown in red. As depicted in Fig. 6A, the FACS analysis measured the level of auto fluorescence of approximately 0.01% for the brain control sections. FACS analysis of fluorescently labelled SNPs (batches Ru@Glu-SNPs and Ru@Glu-PEG-SNPs) as presented in Fig. 6A and 6B, revealed significant fluorescence intensity of about 98.10% and 99.11%, respectively, and were considered as 100% controls.

In the subsequent experiments the uptake efficiency of both, unmodified (Ru@Glu-SNPs) and PEG-SNPs (Ru@Glu-PEG-SNPs), was compared after 1 h of administration. The internalized SNPs in the brain tissues displayed in FACS analysis dotted fluorescence of significant magnitude of about 1.41% and 1.60%, respectively, when compared to the control sections. The brain uptake of PEG modified SNPs increased over 0.8-fold in comparison to glucose coated SNPs, probably to the surface features known to enforce cell adhesion and cellular uptake (Langiu et al., 2014). We assume that one possible mechanism for the uptake of glucose coated SNPs occurs via an active absorptive-mediate endocytosis together with GLUT protein-carrier-mediated transport, processes that cannot be completely excluded for the PEG-amino functionalized SNPs. Due to the positive charge of PEG surrounding molecule, the nanoparticles are able to cross the BBB also through microvascular transport proteins interactions, such as apoE and the low density lipoprotein (LDL) receptor-mediated pathway as previously discussed (Gref et al., 2000). Therefore, the significant level of multi-shell SNPs reaching

the brain demonstrates the high penetration rate of it through BBB.

3.3. TEM

Ultra-thin sections of mice brains were examined by TEM after nanoparticles administration in order to further confirm the SNPs penetration across the BBB and to investigate their distribution in cerebral tissues. The Ru@Glu-PEG-SNPs were chosen for the TEM visualization due to their higher uptake rate according to the biodistribution studies discussed in the previous section. The acquired TEM images confirmed that the SNPs crossed the BBB and were present in different parts of the brain at the observed time point (1 h post-administration) (Fig. 7). According to the obtained images, the PEGylated SNPs reached the cytoplasm of vascular endothelial cells, the astrocytes and probably the neurons in the cerebral parenchyma, also visualized by Ku et al. (2010). Fig. 7 shows also the integrity of the endothelial junction and membrane, therefore the BBB was surmountable probably by transcytosis of vascular endothelial cell. However, the real challenge lies in how surface moieties have the possibility of BBB disruption for an effective targeting (Ku et al., 2010; Poduslo and Curran, 1996).

Also, the ultrastructural localization and morphology of SNPs were visualized by TEM observation. Fig. 5 shows Ru@Glu-PEG-SNPs (in dark) surrounded by light brain cells. The spheres visualized in Fig. 7 ranged from 50 to 100 nm in diameter with several areas of agglomeration of approximately 500 nm in diameter, indicating a multi-level self-arrangement
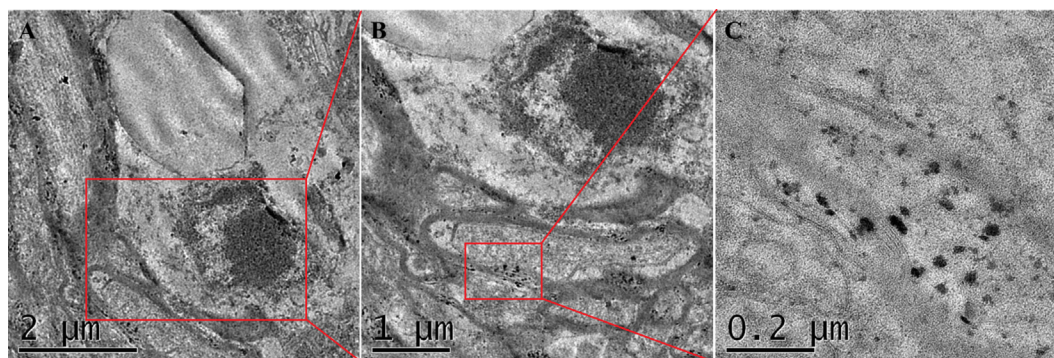
Fig. 7 TEM representative omicrographs of brain sections sacrificed 1 h post-injection with PEGylated SNPs (batch Ru@Glu-PEG-SNPs).

of PEGylated SNPs due to the interactions with the proteins present in the nervous system, also observed in a previous published paper (Rocha et al., 2011).

4. Conclusions

The findings in this work points out the potential application of nanosized engineered SNPs derivatives in the delivery of therapeutic agents across the BBB. Spherically shaped with smooth surface SNPs of about 70 nm determined by FE-SEM analysis were successfully synthesized by reverse microemulsion method followed by glucose and PEG-NH$_2$ molecules surface anchorage. The presence of both glucose and PEG-amino moieties on the nanoparticle's surface promoted their uptake by brain cells in different percentages. The Glu-SNPs and Glu-PEG-NH$_2$-SNPs administered intraperitoneally passed the BBB, and entered the cytoplasm of vascular endothelial cells, as depicted by the biodistribution studies, flow cytometry analysis and subcellular TEM micrographs. The mechanism for the brain uptake of the nanoparticles appeared to be receptor-mediated endocytosis by the endothelial cells of the brain capillary followed by transcytosis and ApoE, LDL and GLUT transporters support. This paper opens new opportunities of applying these innovative nanovehicles for drug delivery and imaging for brain diseases due to their versatile functions of linking different molecules to the same core. Further studies will be performed in order to understand and clarify the mechanisms which control the carrier-mediated transport of the multifunctional SNPs to the brain.

Limitations and implications: in order to ensure that the authors provide accurate context for the present work and give reader's sufficient information to properly evaluate the relevance and impact of the positive obtained results, possible identified limitations are included. These are the study design of the SNPs with the limitation being developed only on mice and statistical or data limitations in accordance with the ethical committee to use a limited number of animals.

Acknowledgement

Conflict of interest

The authors declare they have no competing interests. There is no conflict of interest of any type in the reporting of these data relative to any author.

References

Abbott, N.J., Ronnback, L., Hansson, E., 2006. Astrocyte-endothelial interactions at the blood-brain barrier. Nat. Rev. Neurosci. 7, 41–53.

Alexa, T., Luca, A., Dondas, A., Bohotin, C.R., 2015. Preconditioning with cobalt chloride modifies pain perception in mice. Exp. Ther. Med. 9, 1465–1469.

Balan, V., Verestiuc, L., 2014. Strategies to improve chitosan hemocompatibility: A review. Eur. Polym. J. 53, 171–188.

Barua, S., Mitragotri, S., 2014. Challenges associated with penetration of nanoparticles across cell and tissue barriers: a review of current status and future prospects. Nano Today 9, 223–243.

Bharadwaj, V.N., Nguyen, D.T., Kodibagkar, V.D., Stabenfeldt, S.E., 2018. Nanoparticle-based therapeutics for brain injury. Adv. Healthcare Mater. 7, 1700668.

Caruso, G., Caffo, M., Alafaci, C., Raudino, G., Cafarella, D., Lucerna, S., Salpietro, F.M., Tomasello, F., 2011. Could nanoparticle systems have a role in the treatment of cerebral gliomas? Nanomedicine 7, 744–752.

Chen, Y., Liu, L., 2012. Modern methods for delivery of drugs across the blood-brain barrier. Adv. Drug Deliv. Rev. 64, 640–665.

Craparo, E.F., Bondì, M.L., Pitarresi, G., Cavallaro, G., 2011. Nanoparticulate systems for drug delivery and targeting to the central nervous system. CNS Neurosci. Ther. 17, 670–677.

Cupaioli, F.A., Zucca, F.A., Boraschi, D., Zecca, L., 2014. Engineered nanoparticles. How brain friendly is this new guest? Prog. Neurobiol. 20, 119–120.

Das, S., Carnicer-Lombarte, A., Fawcett, J.W., Bora, U., 2016. Bio-inspired nano tools for neuroscience. Prog. Neurobiol. 142, 1–22.

Feng, Y., Panwar, N., Hang Tng, D.J., Chuan Tjin, S., Wang, K., Yong, K.T., 2016. The application of mesoporous silica nanoparticle family in cancer theranostics. Coord. Chem. Rev. 319, 86–109.

Fiandra, L., Colombo, M., Mazzucchelli, S., Truffi, M., Santini, B., Allevi, R., 2015. Nanoformulation of antiretroviral drugs enhances their penetration across the blood brain barrier in mice. Nanomedicine 11, 1387–1397.

Fornaguera, C., Dols-Perez, A., Calderó, G., García-Celma, M.J., Camarasa, J., Solans, C., 2015. PLGA nanoparticles prepared by nano-emulsion templating using low-energy methods as efficient nanocarriers for drug delivery across the blood-brain barrier. J. Control Release. 211, 134–143.

Georgieva, J.V., Hoekstra, D., Zuhorn, I.S., 2014. Smuggling drugs into the brain: an overview of ligands targeting transcytosis for drug delivery across the blood–brain barrier. Pharmaceutics 6, 557–583.

Gomes, J.M., Mendes, B., Martins, S., Sarmento, B., 2016. Cell-based in vitro models for studying blood-brain barrier (BBB) permeability, in Concepts and models for drug permeability studies. Elsevier, 169–188.

Gref, R., Lück, M., Quellec, P., Marchand, M., Dellacherie, E., Harnisch, S., Blunk, T., Müller, R.H., 2000. 'Stealth' corona-core nanoparticles surface modified by polyethylene glycol (PEG): influences of the corona (PEG chain length and surface density) and of the core composition on phagocytic uptake and plasma protein adsorption. Colloids Surf. B: Biointerfaces 18, 301–313.

Grover, A., Hirani, A., Sutariya, V., 2013. Nanoparticle-based brain targeted delivery systems. J. Biomol. Res. Ther. 2, e113.

Hanada, S., Fujioka, K., Inoue, Y., Kanaya, F., Manome, Y., Yamamoto, K., 2014. Cell-based in vitro blood-brain barrier model can rapidly evaluate nanoparticles' brain permeability in association with particle size and surface modification. Int. J. Mol. Sci. 15, 1812–1825.

Jiang, X., Xin, H., Ren, Q., Gu, J., Zhu, L., Du, F., Feng, C., Xie, Y., Sha, X., Fang, X., 2014. Nanoparticles of 2-deoxy-D-glucose functionalized poly (ethylene glycol)-co-poly (trimethylene carbonate) for dual-targeted drug delivery in glioma treatment. Biomaterials 35, 518–529.

Jose, S., Sowmya, S., Cinu, T.A., Aleykutty, N.A., Thomas, S., Souto, E.B., 2014. Surface modified PLGA nanoparticles for brain targeting of Bacoside-A. Eur. J. Pharm. Sci. 63, 29–35.

Kanwar, J.R., Sriramoju, B., Kanwar, R.K., 2012. Neurological disorders and therapeutics targeted to surmount the blood–brain barrier. Int. J. Nanomed. 7, 3259–3278.

Koffie, R.M., Farrar, C.T., Saidi, L.J., William, C.M., Hyman, B.T., Spires-Jones, T.L., 2011. Nanoparticles enhance brain delivery of blood-brain barrier-impermeable probes for in vivo optical and

magnetic resonance imaging. Proc. Natl. Acad. Sci. USA 108, 18837–18842.

Ku, S., Yan, F., Wang, Y., Sun, Y., Yang, N., Ye, L., 2010. The blood–brain barrier penetration and distribution of PEGylated fluorescein-doped magnetic silica nanoparticles in rat brain. Biochem. Biophys. Res. Commun. 394, 871–876.

Lalatsa, K., Barbu, E., 2016. Carbohydrate nanoparticles for brain delivery. Int Rev Neurobiol. 130, 115–153.

Langiu, M., Dadparvar, M., Kreuter, J., Ruonala, M.O., 2014. Human serum albumin-based nanoparticle-mediated in vitro gene delivery. Plos One 9, 107603.

Legrand, S., Catheline, A., Kind, L., Constable, E.C., Housecroft, C. E., Landmann, L., Banse, P., Pieles, U., Wirth-Heller, A., 2008. Controlling silica nanoparticle properties for biomedical applications through surface modification. New J. Chem. 32, 588–593.

Liu, D., Lin, B., Shao, W., Zhu, Z., Ji, T., Yang, C., 2014. *In vitro* and *in vivo* studies on the transport of PEGylated silica nanoparticles across the blood-brain barrier. ACS Appl. Mater. Interfaces 6, 2131–2136.

Mangraviti, A., Gullotti, D., Tyler, B., Brem, H., 2016. Nanobiotechnology-based delivery strategies: new frontiers in brain tumor targeted therapies. J. Control Release 16, S0168–S3659.

Poduslo, J.F., Curran, G.L., 1996. Permeability at the blood-brain and blood-nerve barriers of the neurotrophic factors: NGF, CNTF, NT-3, BDNF. Brain Res. Mol. Brain Res. 36, 280–286.

Rabanel, J.M., Hildgen, P., Banquy, X., 2014. Assessment of PEG on polymeric particles surface, a key step in drug carrier translation. J. Control. Release 185, 71–87.

Rocha, A., Zhou, Y., Kundu, S., González, J.M., Vinson, S.B., Liang, H., 2011. In vivo observation of gold nanoparticles in the central nervous system of Blaberus discoidalis. J. Nanobiotechnol. 9, 1–9.

Saraiva, C., Praca, C., Ferreira, R., Santos, T., Ferreira, L., Bernardino, L., 2016. Nanoparticle-mediated brain drug delivery: overcoming blood-brain barrier to treat neurodegenerative diseases. J. Control Release 235, 34–47.

Silva, G.A., 2008. Nanotechnology approaches to crossing the blood-brain barrier and drug delivery to the CNS. BMC Neurosci. 9, S4.

Singh, R.K., Prasad, D.N., Bhardwaj, T.R., 2015. Synthesis, physicochemical and kinetic studies of redox derivative of bis(2-chloroethylamine) as alkylating cytotoxic agent for brain delivery. Arab. J. Chem. 8, 380–387.

Singh, R.K., Prasad, D.N., Bhardwaj, T.R., 2017. Design, synthesis, chemical and biological evaluation of brain targeted alkylating agent using reversible redox prodrug approach. Arab. J. Chem. 10, 420–429.

Toman, P., Lien, C.F., Ahmad, Z., Dietrich, S., Smith, J.R., An, Q., Molnár, É., Pilkington, G.J., Górecki, D.C., Tsibouklis, J., Barbu, E., 2015. Nanoparticles of alkylglyceryl-dextran-graft-poly(lactic acid) for drug delivery to the brain: preparation and in vitro investigation. Acta Biomater. 23, 250–262.

Voigt, N., Henrich-Noack, P., Kockentiedt, S., Hintz, W., Tomas, J., Sabel, B.A., 2014. Surfactants, not size or zeta-potential influence blood-brain barrier passage of polymeric nanoparticles. Eur. J. Pharm. Biopharm. 87, 19–29.

Wohlfart, S., Gelperina, S., Kreuter, J., 2012. Transport of drugs across the blood-brain barrier by nanoparticles. J. Control Release 161, 264–273.

Zhou, J., Gan, N., Hu, F., Li, T., Zhou, H., Li, X., Zheng, L., 2013. A single antibody sandwich electrochemiluminescence immunosensor based on protein magnetic molecularly imprinted polymers mimicking capture probes. Sens. Actuators B Chem. 186, 300–307.